Engineering and Technology Journal e-ISSN: 2456-3358

Volume 08 Issue 09 September -2023, Page No.- 2740-2756

DOI: 10.47191/etj/v8i9.04, I.F. – 7.136

Effect of Heating and Cooling on 6CB Liquid Crystal Using DSC Technique

Laura Elizabeth Byrne[1], Dr. Dipti Sharma[2]
[1]Undergraduate student, Emmanuel College, Boston, MA, USA
[2]Supervisor Emmanuel College, Boston, MA, USA

ABSTRACT: In this research, details of the heating and cooling of the liquid crystal (LC) 4-cyano-4'-hexylbiphenyl (6CB) were collected through the use of Differential Scanning Calorimetry (DSC), and then analyzed with Logger Pro. The sample of 6CB was heated from -40 °C to 80 °C and then cooled to -40 °C again at a constant rate of 20 °C/min. DSC provided data for the time, temperature, and heat flow, which was used to calculate thermal speed, acceleration, and jerk, as well as the specific heat capacity at each point. Graphs of this data contain endothermic and exothermic peaks that indicate phase transitions, revealing information such as the enthalpy of the peak and the nematic range. One focus of this study was to compare 6CB to other liquid crystals that are part of the n-alkyl-cyanobiphenyl (nCB) family to see if the difference in tail length affects the behavior of the liquid crystal. Results show that 6CB may be of interest as an alternative to other liquid crystals for liquid crystal displays (LCD).

KEYWORDS: Heating, Cooling, Temperature, Heat Flow, Specific Heat Capacity, Time, Thermal Energy, Thermal Speed, Thermal Acceleration, Differential Scanning Calorimetry, 6CB, Phase Change, Peak, Endothermic, Exothermic, Crystalline, Nematic, Isotropic, Logger Pro.

INTRODUCTION

Heating refers to the process of transferring thermal energy from one system to another by increasing its temperature. When a system is heated, the thermal energy is converted to kinetic energy and increases the movement of the molecules within the system. In contrast, cooling refers to the loss of thermal energy from a system and shows less movement in the molecules. When a crystalline material is heated, the increase of kinetic energy causes molecules to lose their ordered alignment and structure. With the addition of heat, the temperature rises until the object undergoes a phase transition. During this phase transition, the temperature remains constant, as the energy is used to break down the intermolecular forces that hold the molecules together. [1-3]

Typical matter has three phases: solid, liquid, and gas. In the solid state, molecules are ordered and more densely packed together, but as they are heated, the bonds between them weaken and the matter enters the liquid state. For example, water in its solid state is ice, which has a fixed shape and volume, but as heat is transferred to the ice, it begins to lose its shape, but the volume remains the same. If more heat is added to the liquid matter, the bonds are further weakened and it becomes a gas, just as water becomes a vapor when boiled. [3]

Liquid Crystals (LCs) are not typical matter and are not limited to having only three states. The molecules that make up the LC can be densely packed and ordered, making it a crystalline solid, and similar to most typical matter, it can be heated until the bonds holding the molecules together have weakened enough to allow the LC to enter its liquid phase, known as the isotropic state. However, LCs can also exist in a state between crystalline and liquid, such as the nematic phase, where it is not quite solid or liquid. In this phase, the molecules, which are often elongated in shape, remain mostly vertical and facing in the same direction on average, but without positional order. LCs in the crystalline phase can be heated until they reach the nematic phase, and if heated further, they will reach the isotropic phase. This change is only physical, rather than chemical, so just as water that has been frozen can melt again, an LC that has been crystallized or melted can still be heated or cooled to return to its previous phase. LCs that undergo phase transitions due to heating or cooling are known as thermotropic, and due to their unique ability to be manipulated by electrical currents, they have been used to create Liquid Crystal Displays (LCDs), often used for laptops, televisions, smart phones, and more. In order to analyze phase transitions in thermotropic LCs, a technique known as differential scanning calorimetry (DSC) can be employed. [4-11]

DSC is a technique that helps to find phase changes of matter using thermodynamics. In DSC, the instrument transfers energy to the sample in the form of heat, reaching a specified temperature using a chosen ramp rate, and then cools the sample to the beginning temperature. At the same time, a reference material is heated and cooled in the same instrument in a separate compartment. The sample and reference material are kept at the same temperature as each other throughout; therefore, if the sample undergoes a phase transition, the instrument will need to provide more heat to keep the rate of temperature change the same. [12-15]

The material of focus in this research is 4-cyano-4'-hexylbiphenyl (6CB), a member of the n-alkyl-cyanobiphenyl (nCB) family of thermotropic LCs. These molecules all consist of two phenyl groups connected by a single bond, a cyano group head, and a carbon chain tail. The number of carbons in this chain is signified by the value attributed to n, therefore 6CB contains six carbons in its tail. The intention of this study is to examine the phase transitions of 6CB by using DSC, and to compare its behavior to that of other LCs in the nCB family, such as 4CB or 10CB, which have a shorter and longer tail than 6CB, respectively. [16-19] The molecular structure of 6CB, which causes its elongated shape, can be seen in Figure 1.

In order for LCs to be useful in LCD, they often must be in the nematic phase. Therefore, it is important to know the nematic range of the LC. The wider the range, the more practical the LC is, so that the display can withstand changes in temperature. By analyzing the phase transitions of 6CB, the nematic range when being heated and cooled can be found and compared to other members of its nCB family. [20-21] A comparison between nCB members is shown in Figure 2. Whether the LC has an even or odd number of carbons in its tail determines the direction in which the tail points. Additionally, the molecular arrangement of 6CB in the Crystalline, Nematic, and Isotropic phases is illustrated in Figure 3.

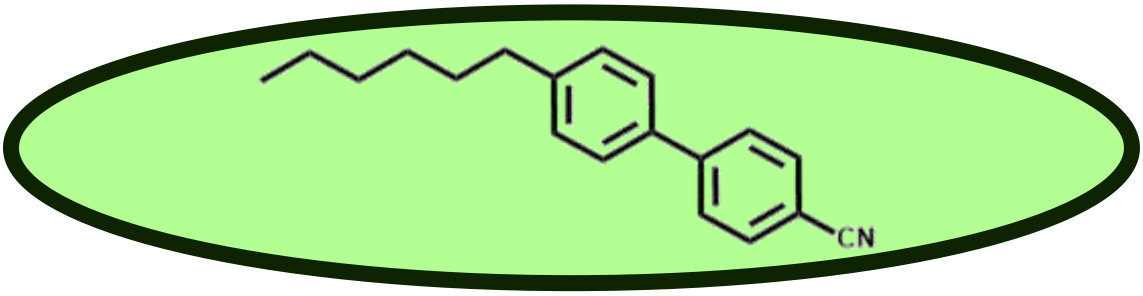

Figure 1. The molecular structure of 6CB, shows the molecule's rod-like shape.

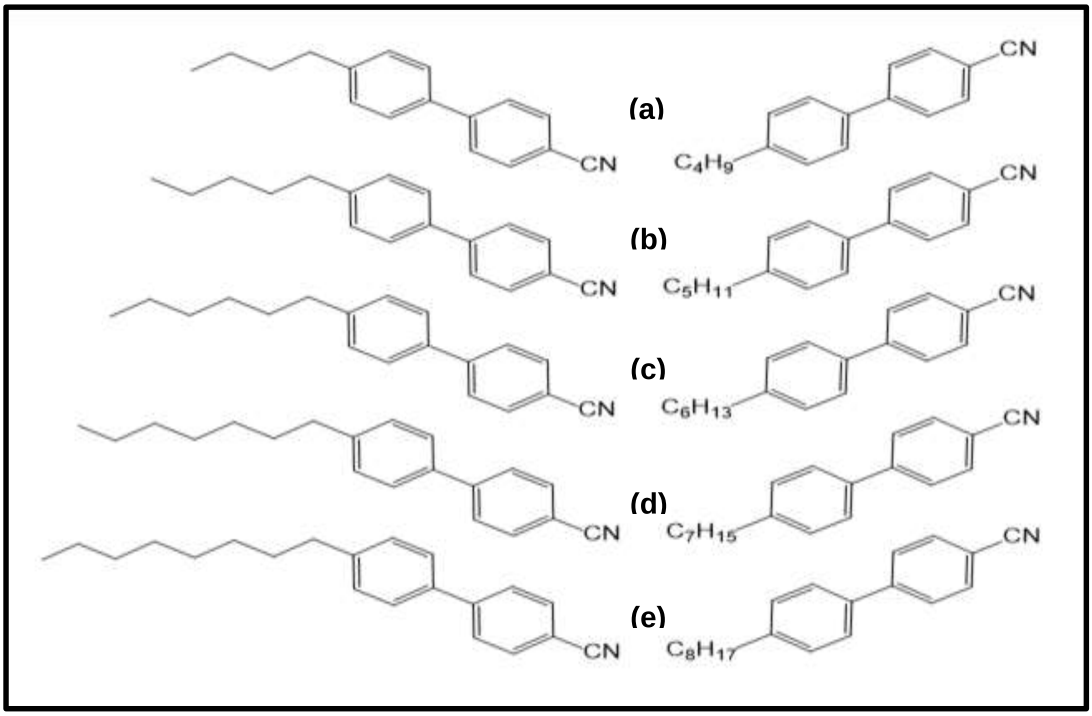

Figure 2. Visual comparison of the structure and varying tail lengths of LCs from the nCB family, including (a) 4CB, (b) 5CB, (c) 6CB, (d) 7CB, and (e) 8CB.

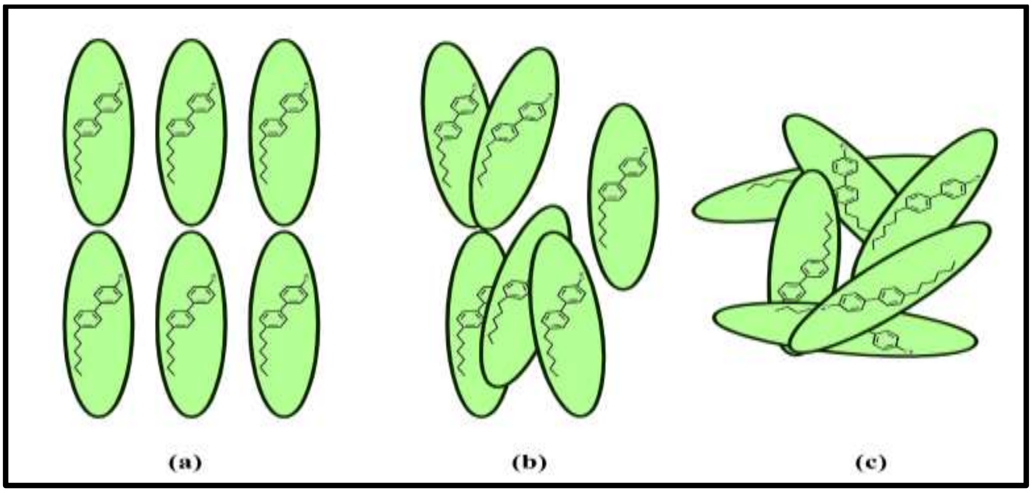

Figure 3. Arrangement of 6CB molecules in the (a) crystalline, (b) nematic, and (c) isotropic phases.

MATERIAL AND THEORY

In this research, pure 4-hexyl-4'-cyanobiphenyl (6CB) liquid crystal, also referred to as 4′-hexyl-4-biphenylcarbonitrile or 4-cyano-4′-hexylbiphenyl, was run in a Differential Scanning Calorimetry (MDSC 2920) from TA instruments at WPI. Data was collected in DSC and then analyzed further using Logger Pro.

LCs follow the laws of thermodynamics, and the DSC instrument works on the concept of thermodynamics. The related theory as involved in this research can be seen below:

During heating and cooling, when temperature is changed, the heat going in or coming out (Q) can be related to the mass of the substance (m), specific heat of capacity (Cp) and temperature change (ΔT) as

$$Q = m*Cp*\Delta T \qquad — 1$$

When a material goes through a phase change without changing the temperature of the substance, heat given to the substance (Q) can be related to the mass of the substance (m) and latent heat of the phase change (L) as

$$Q = m*L \qquad — 2$$

When phase change and temperature change both take place, we can combine these two equations,

$$Q = m*Cp*\Delta T + m*L \qquad — 3$$

Using DSC technique, heat flow can be given as a function of temperature and heating rate,

$$HF = dQ/dt = m*Cp* dT/dt \qquad — 4$$

Specific heat capacity of the substance can be found as

$$Cp = (1/m)*[(dQ/dt)/(dT/dt)] \qquad — 5$$

The heat flow of the 6CB liquid crystal system can be used to find thermal speed, thermal acceleration, and thermal jerk during heating and cooling. The thermal speed can be written as

$$d(HF)/dt = (dQ/dt)' = [(d^2)(Q)]/(dt^2) \qquad — 6$$

Thermal acceleration can be found as the first derivative of equation 6, or the second derivative of equation 4, shown in equation 7.

$$[d^2(HF)]/(dt^2) = (dQ/dt)'' = [(d^3)(Q)]/(dt^3) \qquad — 7$$

Thermal jerk can be found as the first derivative of equation 7, the second derivative of equation 6, or the third derivative of equation 4, shown in equation 8.

$$[d^3(HF)]/(dt^3) = [(d^4)(Q)]/(dt^4) \qquad — 8$$

EXPERIMENTS

The 4-hexyl-4-cyanobiphenyl (6CB) has a molecular weight of 263.38 g/mol and is nematic at room temperature. The bulk sample was placed in the DSC instrument to study its thermal and phase transition details. For calorimetric experiments, a small amount of 6CB was loaded into pans, sealed with lids using a DSC press, and then placed inside a DSC instrument. The heating and cooling of the 6CB is done from -40 °C to 80 °C and then from 80 °C to -40 °C at a constant heating and cooling rate of 20 °C/min. The respective heat flow of the samples was recorded along with temperature change during the heating and cooling scans.

DSC results show that when 6CB is heated, it forms one large endothermic peak and one small endothermic peak on heating and then a small exothermic peak, and a large exothermic peak and a small exothermic peak in cooling. These peaks correspond to a Crystalline to Nematic peak, K-N (large peak) and a Nematic to Isotropic peak, N-I (small peak) on heating and cooling.

RESULTS

The data obtained from the DSC was analyzed using Logger Pro in order to study the phase transitions and properties of the LC 6CB, depicted in Figures 4-22. The data was first plotted as heat flow (W/g) versus temperature (℃), as seen in Figure 4, showing the heating and cooling of the sample of 6CB. The first phase transition is indicated by the large endothermic peak at 17.45 ℃, soon followed by a smaller peak at 30.27 ℃. These peaks represent the transitions from crystalline to nematic, then nematic to isotropic. The sample remains in the isotropic state as it is heated further, represented by the mostly flat line. The sample then transitions back to nematic as it is cooled, forming a small exothermic peak at 26.85 ℃, and remaining nematic until its second, larger, exothermic peak at 0.46 ℃.

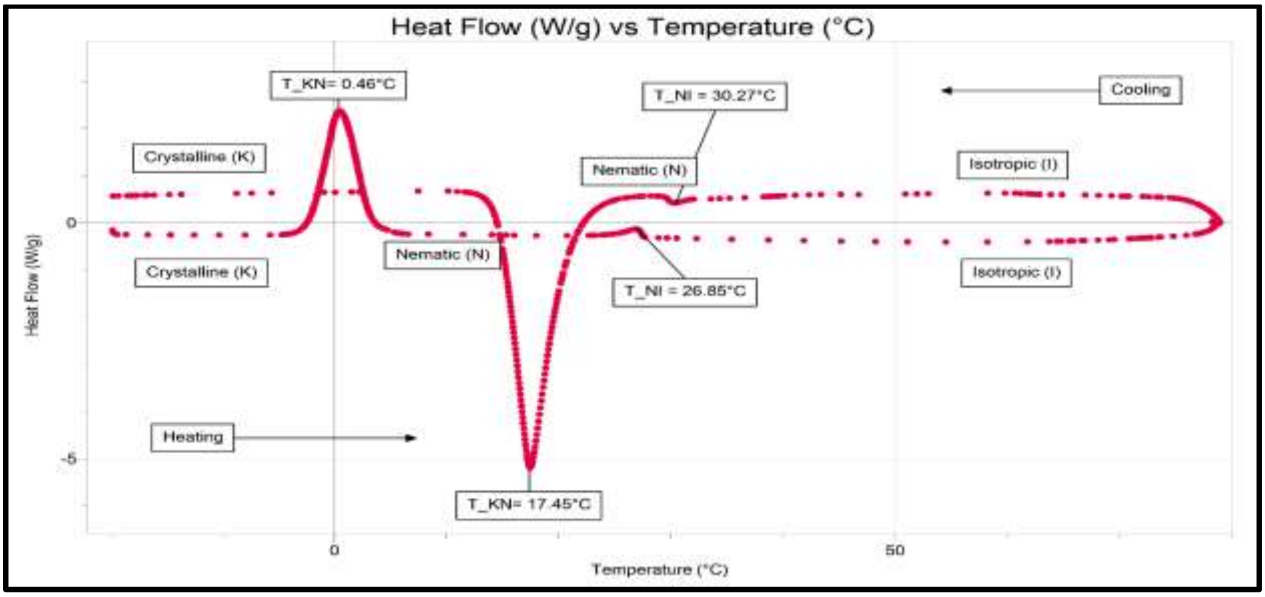

Figure 4. Heat Flow, HF (W/g) vs Temperature, T (℃) of 6CB being heated from crystalline to nematic, then to isotropic, and cooled from isotropic to nematic, then to crystalline.

The values of heat flow provided by the DSC instrument were used to calculate the specific heat capacity of the sample at each temperature, as seen in Figure 5. The thermal energy used by the sample of 6CB is represented by the pink shaded area, which is the integral of the plot. As the sample is heated and cooled, its internal energy changes because it is absorbing and releasing thermal energy. The internal energy was calculated to be 169.3 J/g using Logger Pro.

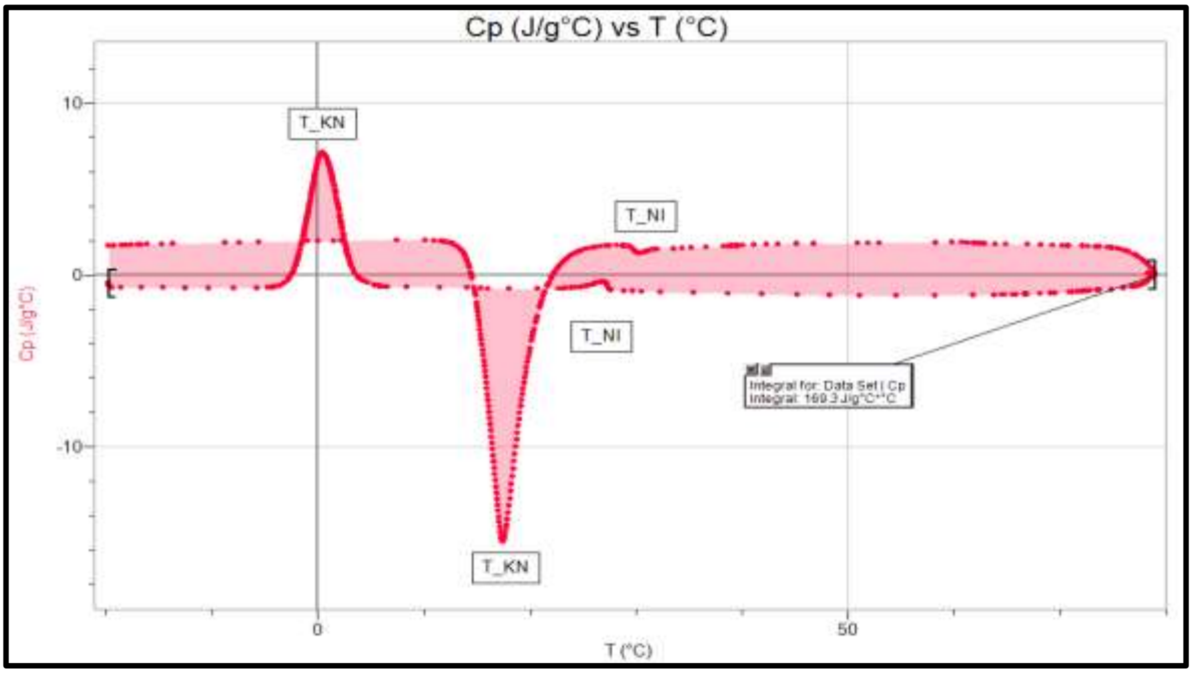

Figure 5. Specific Heat Capacity, Cp (W/g) vs Temperature, T (℃) of 6CB being heated and cooled. The pink shaded area shows the integral.

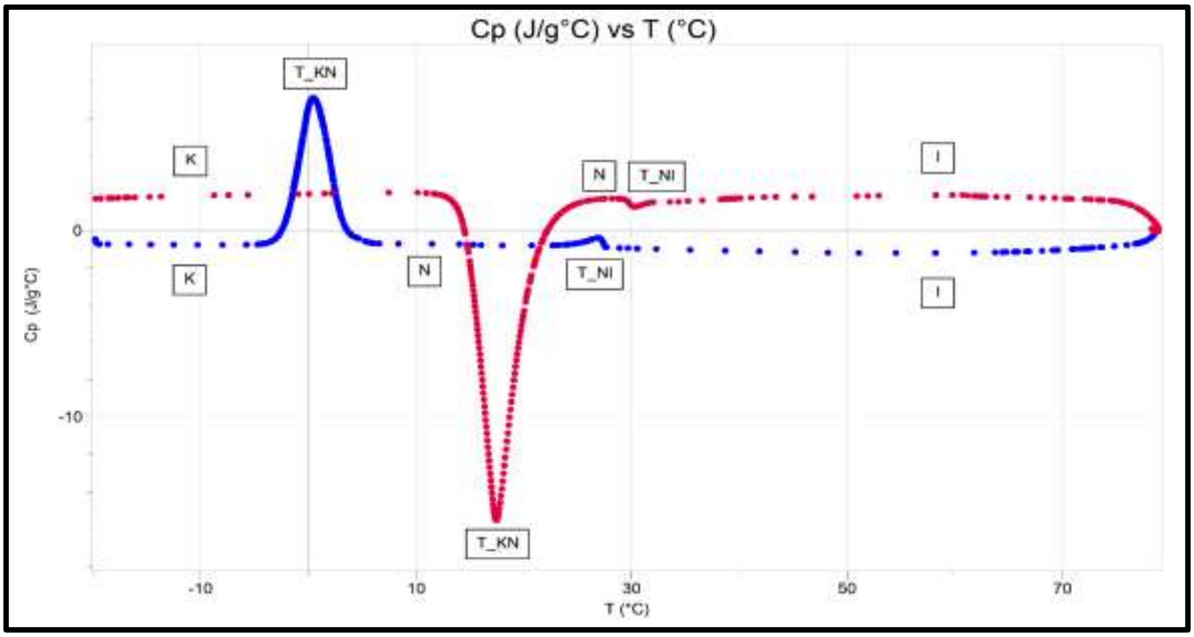

Figure 6. Cp (J/g°C) vs T (°C) of 6CB being heated from crystalline to nematic, then to isotropic, and cooled from isotropic to nematic, then to crystalline.

The heating and cooling of 6CB can be seen more clearly in Figure 6, with the red datapoints and downward peaks indicating when the sample is being heated, while the blue datapoints and upward peaks show when the sample is being cooled. With the exception of the crystalline-nematic phase transitions, labeled T_KN, the specific heat capacity of the sample is higher when it is being heated than when it is being cooled.

Focusing specifically on the heating of 6CB, as shown in Figure 7, the two endothermic transitions can be seen more clearly. The sample begins in the crystalline state, but as kinetic energy is transferred to the molecules in the form of heat, they start to lose order and begin to undergo the K-N phase transition. At T_KN, the sample is about half crystalline and half nematic, and as the specific heat capacity rises from this point, the amount of nematic sample increases until it is fully nematic. The sample remains in the nematic state for a short time until the next, much smaller, endothermic peak at T_NI, where the sample is becoming isotropic

.

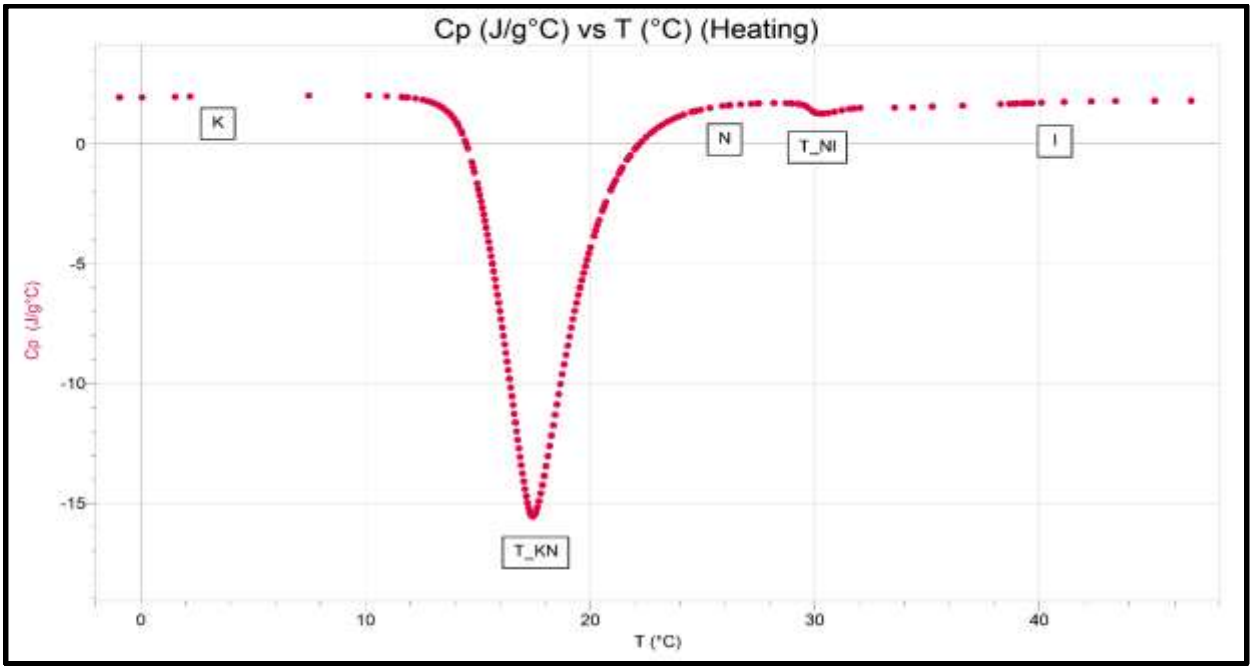

Figure 7. Cp (J/g°C) vs T (°C) of 6CB being heated from crystalline (K) to nematic (N) and then to isotropic (I), between 0 °C and 45 °C.

The zoomed-in plot of the cooling of 6CB, seen in Figure 8, shows the sample beginning in the isotropic phase, where it releases heat, reaching the peak labeled T_NI. At this point, around half of the sample is still in the isotropic phase, while the other half has entered the nematic phase. The sample remains in the nematic state as it loses more energy in the form of heat, until the second, much larger, exothermic peak at T_KN, at which half of the sample is still nematic, and half is crystalline. The specific heat capacity of the sample shows a slight overall increase from before the I-N and N-K phase transitions to after.

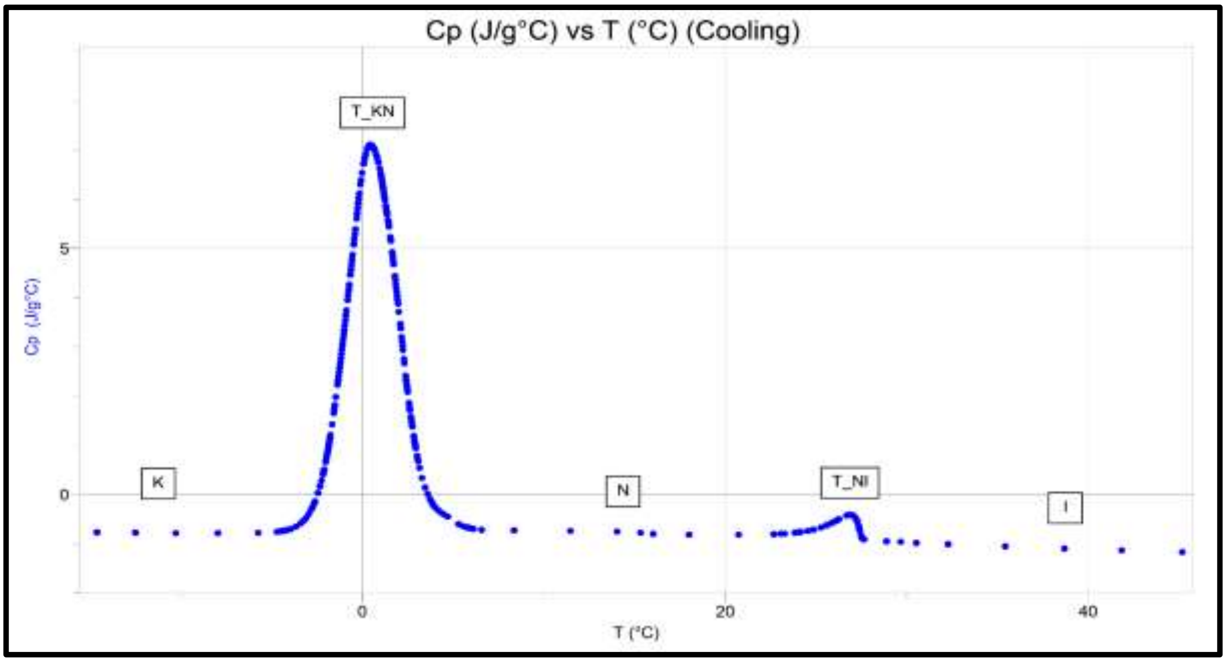

Figure 8. Cp (J/g°C) vs T (°C) of 6CB being cooled from isotropic (I) to nematic (N) to crystalline (K) between around -20 °C and 45 °C.

In Figures 9-12, Ts, Te, and ΔT mark the starting temperature, end temperature, and the overall change in temperature. Cps, Cpe, and Cpp mark the beginning specific heat capacity, end specific heat capacity, and specific heat capacity at the peak of the transition. CpJ represents the wing jump of the transition. These labels are also defined in Tables 1 and 2.

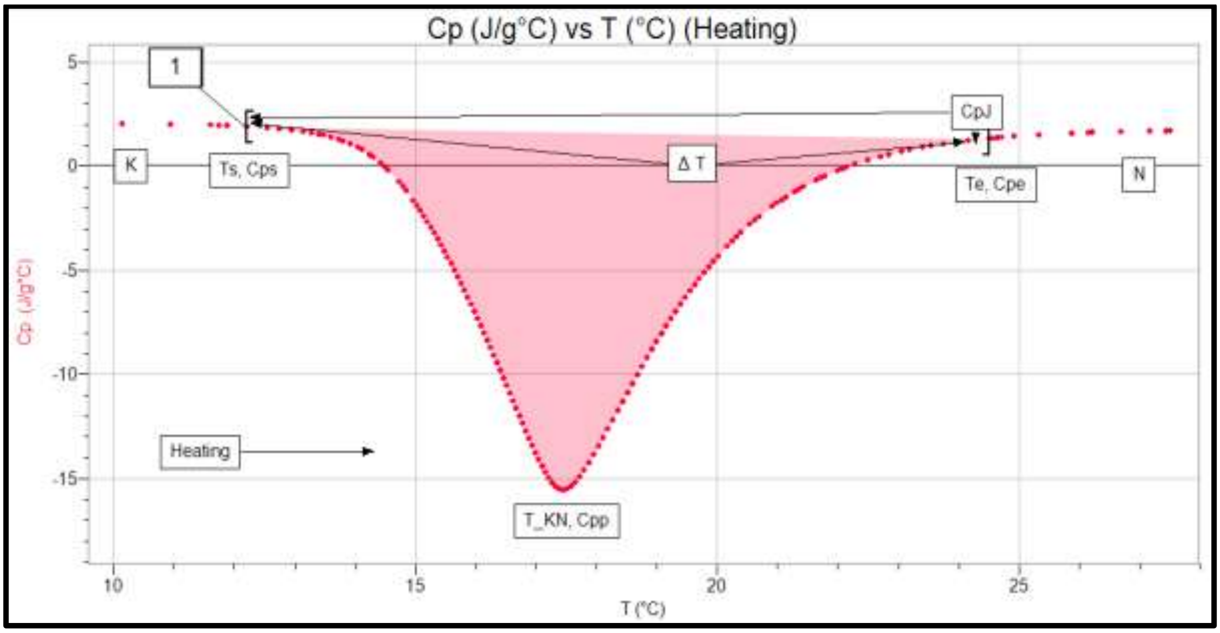

Figure 9. Cp (J/g°C) vs T (°C) of 6CB being heated from crystalline (K) to nematic (N). The pink shaded area shows the integral of the peak.

Figure 9 focuses on the first endothermic peak, showing the phase transition from crystalline to nematic. The peak was integrated using Logger Pro, which resulted in an enthalpy of 66.09 J/g and is depicted by the pink shaded area of the plot. This value represents the internal energy of the sample as it absorbed thermal energy during its K-N transition. There was little change in the overall heat capacity before and after the transition.

The next phase transition of 6CB was also integrated, resulting in an enthalpy of 0.65 J/g, meaning the sample absorbed much less energy while transitioning from nematic to isotropic than it did in its transition from crystalline to nematic. More energy is required in the K-N phase transition because when the LC is in the solid state, its molecules form a crystal lattice, and the intermolecular forces that are present need to be weakened. However, in the N-I phase transition, these forces have already been weakened and the molecules in the nematic state are already somewhat disordered, requiring little additional energy. Furthermore, the zoomed-in plot shows a noticeable wing jump, where the specific heat capacity is higher in the nematic phase than in the isotropic phase, shown in Figure 10.

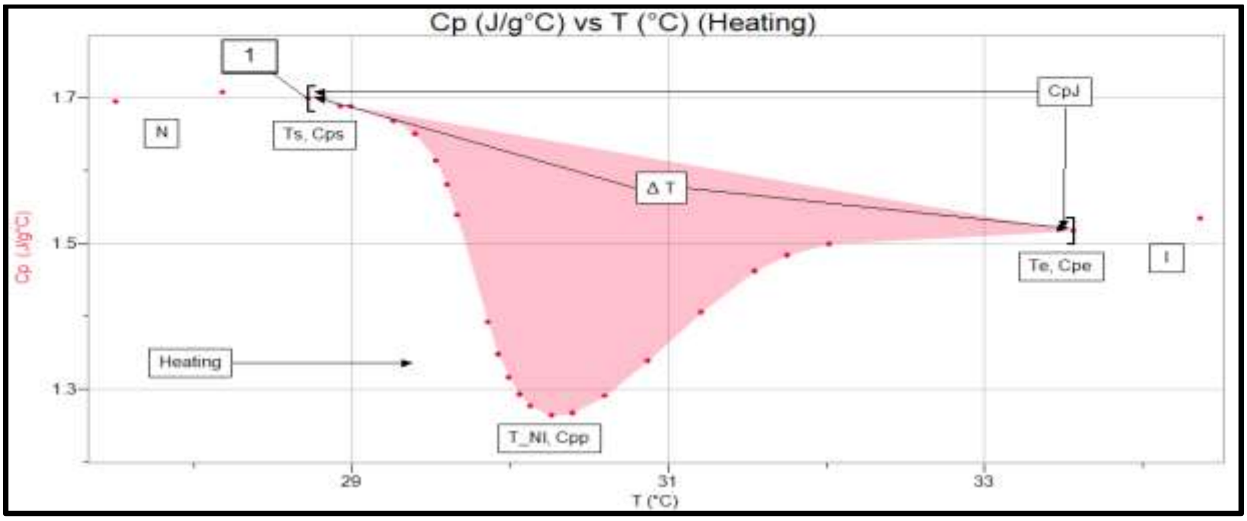

Figure 10. Cp (J/g°C) vs T (°C) of 6CB being heated from nematic (N) to isotropic (I). The pink shaded area shows the integral of the peak.

Figure 11 shows the first exothermic peak that appears during the cooling of 6CB. Peak integration reveals that the enthalpy of this transition from isotropic to nematic is 0.98 J/g, which represents the release of energy that takes place as the sample reaches a lower temperature. The integral of the peak is indicated by the light blue shaded area of the plot. The wing jump shows that the specific heat capacity is higher when the sample is in the nematic state than in the isotropic state.

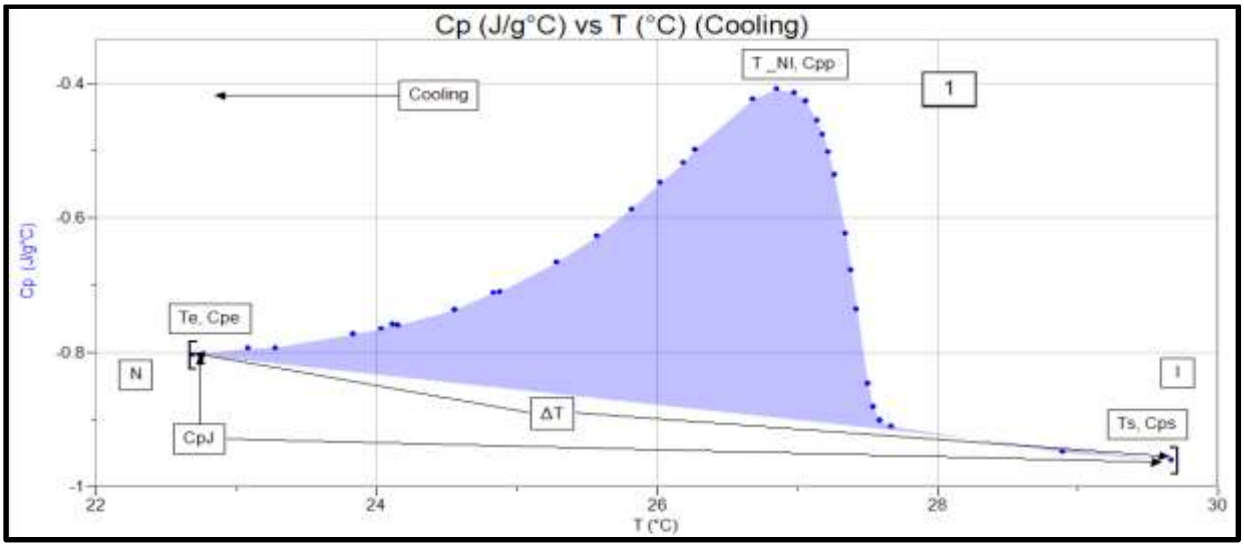

Figure 11. Cp (J/g°C) vs T (°C) of 6CB being cooled from isotropic (I) to nematic (N). The blue shaded area shows the integral of the peak.

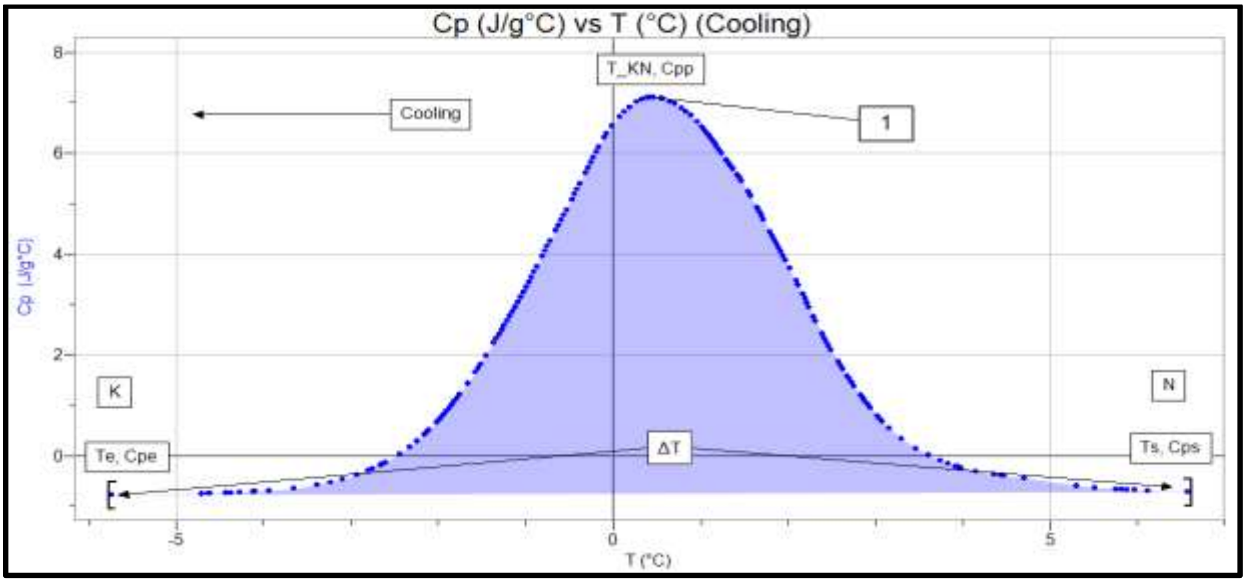

Figure 12. Cp (J/g°C) vs T (°C) of 6CB being cooled from nematic (N) to crystalline (K). The blue shaded area shows the integral of the peak.

The larger exothermic peak, seen in Figure 12, which represents the transition from nematic to crystalline, had an enthalpy of 27.31 J/g, meaning more energy was released in the N-K phase transition than in the I-N phase transition. The molecules must lose kinetic energy in order to regain and maintain order, but as both the isotropic and nematic states are not fully ordered, less energy needs to be lost for the I-N transition. The peak is relatively even and smooth.

Figure 13 shows the heat flow, provided by the DSC instrument, as the sample of 6CB was heated and cooled during its run of about 18 minutes. The downward peaks that appear at the beginning of the plot signify at what point the sample was being heated, while the upward peaks show where the sample was being cooled. The time of each phase transition was determined using this graph and is recorded in Table 6.

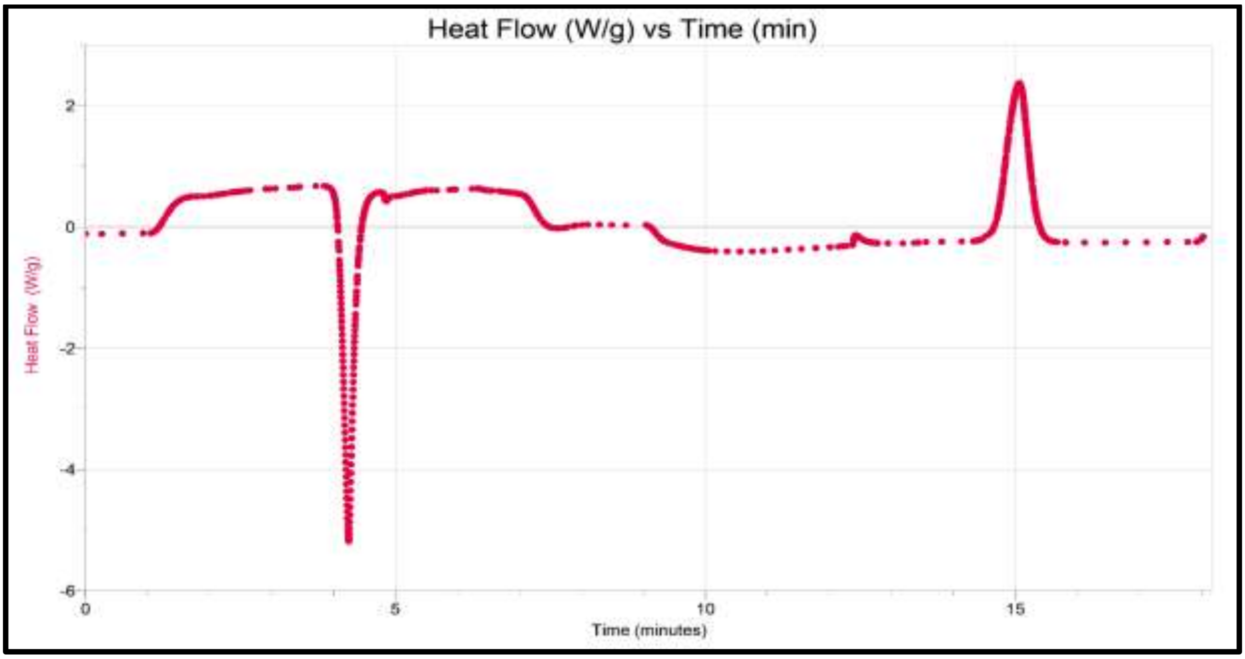

Figure 13. Heat Flow (W/g) vs Time (minutes) of 6CB being heated and cooled.

In order to calculate the thermal speed of the sample, the first derivative of the heat flow (W/g) versus time (min) was taken, as depicted in Figure 14. The thermal speed is relatively stable at zero until a phase transition occurs, which is indicated by the peaks. Similarly, the second derivative of the heat flow is shown by Figure 15, which is equal to the thermal acceleration. The third derivative, in Figure 16, is equal to the jerk. Each graph follows a general pattern of having one large peak followed quickly by a smaller peak, after which the plot flatlines until reaching another small peak and then a medium sized peak. The first two peaks show where heating takes place, with the large peak representing the transition from crystalline to nematic and the smaller peak representing nematic to isotropic. The last two peaks show the transition from isotropic to nematic, and then nematic to crystalline.

.

These graphs show that the thermal energy moves faster and accelerates quicker during the K-N heating phase transition, as the instrument transfers heat to the sample

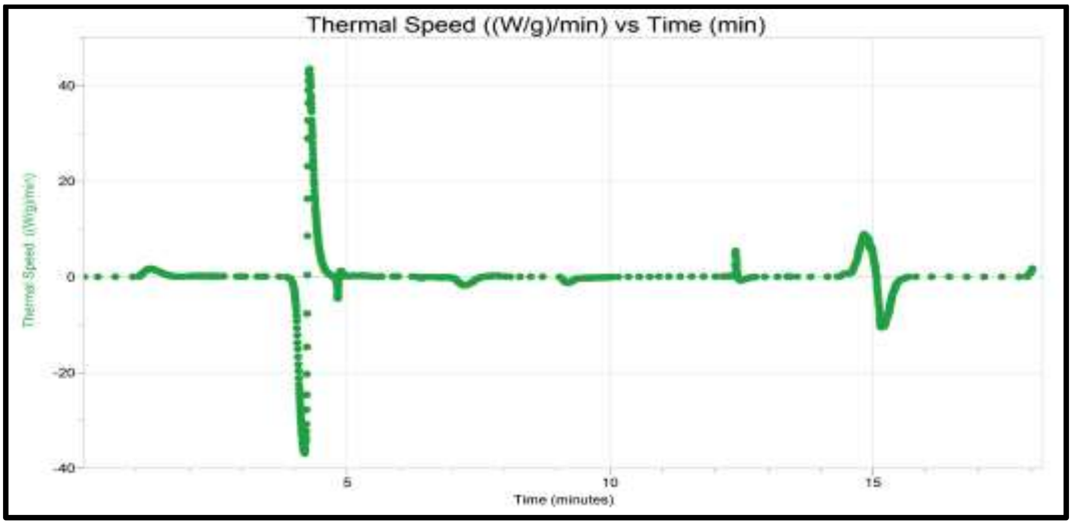

Figure 14. Thermal Speed ((W/g)/min) vs Time (min) of the heating and cooling of 6CB.

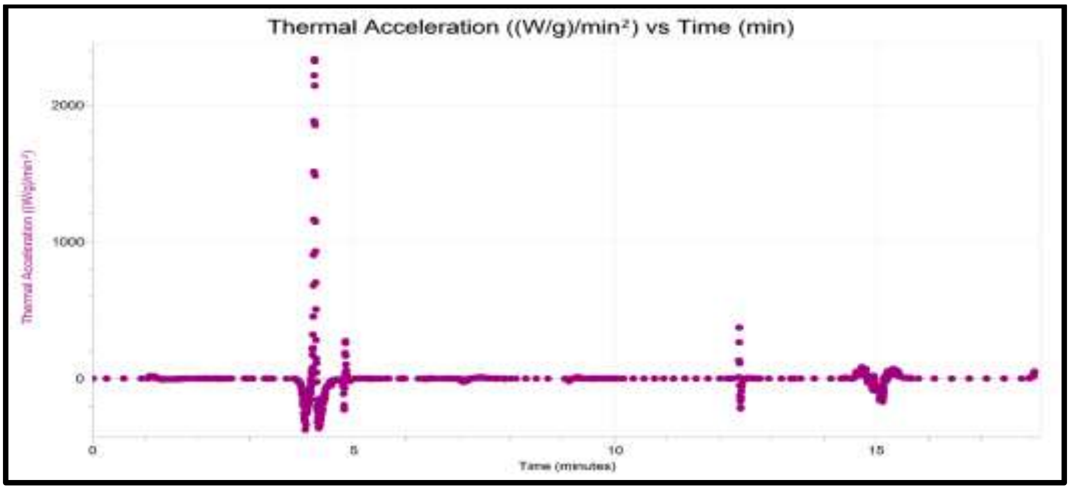

Figure 15. Thermal Acceleration ((W/g)/min^2) vs Time (min) of the heating and cooling of 6CB.

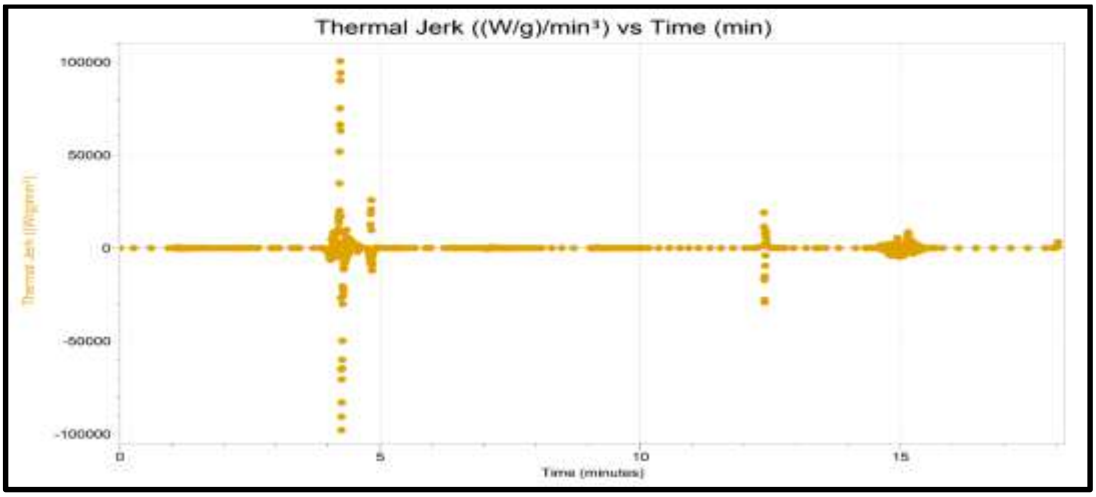

Figure 16. Thermal Jerk ((W/g)/min^3) vs Time (min) of the heating and cooling of 6CB.

Next, the derivative of heat flow (W/g) versus temperature (°C) during the heating of 6CB was calculated, giving the plot in Figure 17. The crystalline to nematic phase transition is indicated by the large, broad curve in the middle of the plot, while the nematic to isotropic phase transition forms a much smaller peak at around 30 °C. The second and third derivatives of heat flow (W/g) versus temperature (°C) during heating were also calculated, as seen in Figures 18 and 19, respectively. Similar to Figure 17, these plots show one large peak during the K-N phase transition and then a much smaller peak indicating the N-I phase transition. In the second derivative, the K-N peak is mostly positive, but in the third derivative the K-N peak is positive and negative. In each plot, the peaks only appear when a phase transition is taking place.

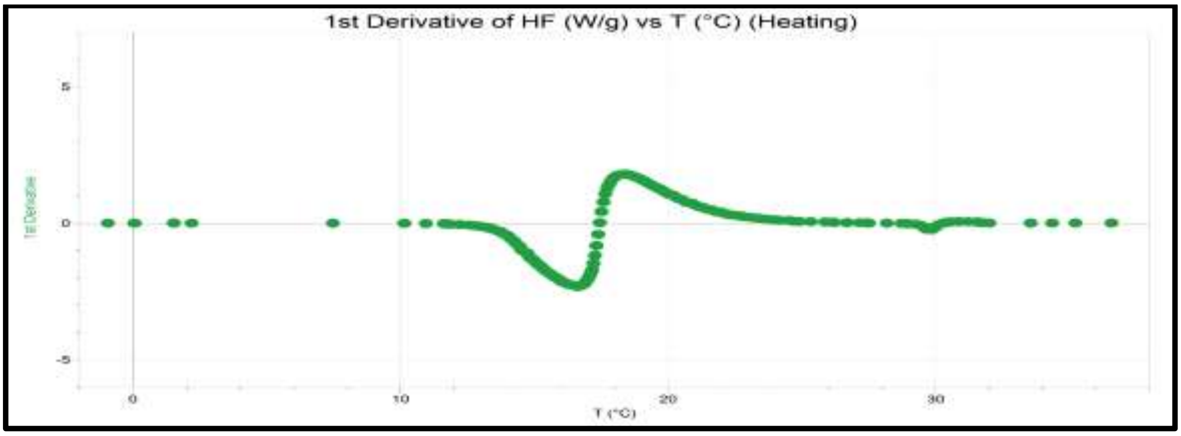

Figure 17. 1st Derivative of HF (W/g) vs T (°C) during the heating of 6CB.

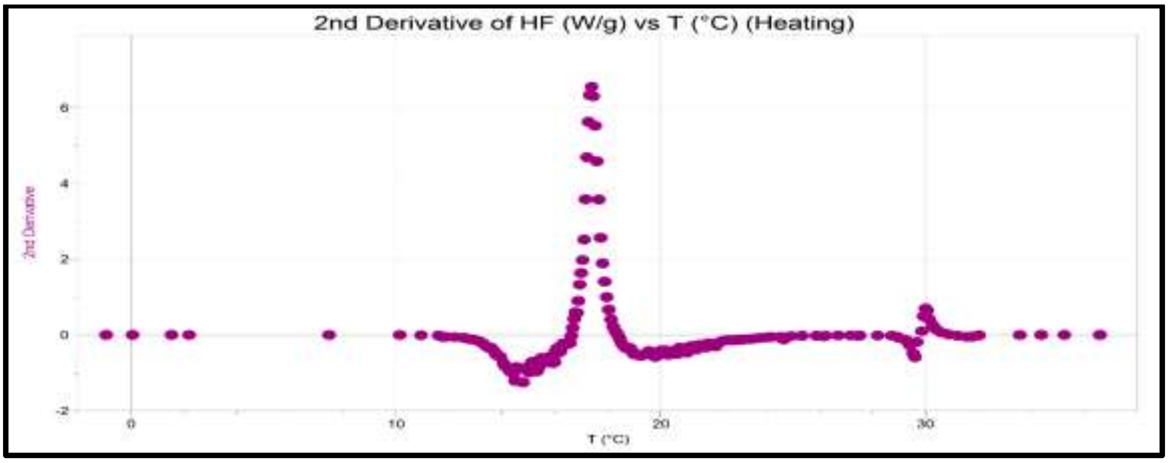

Figure 18. 2nd Derivative of HF (W/g) vs T (°C) during the heating of 6CB.

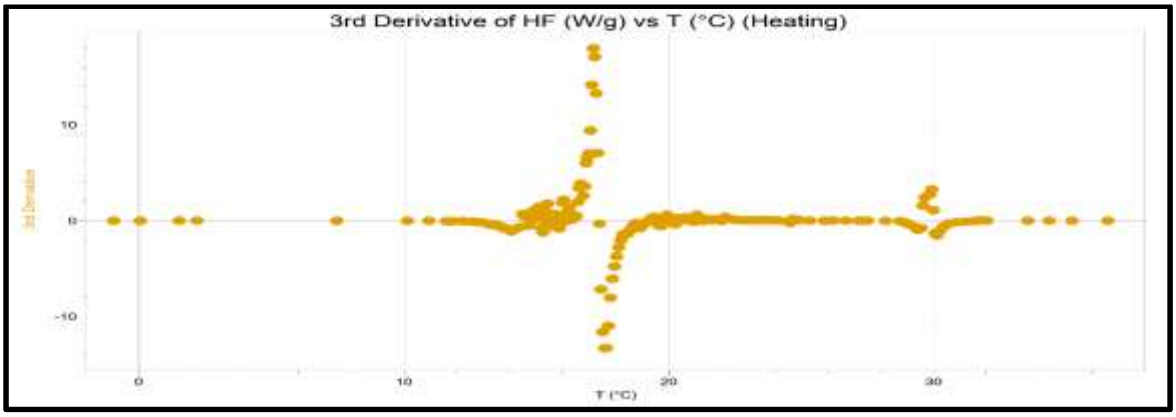

Figure 19. 3rd Derivative of HF (W/g) vs T (°C) during the heating of 6CB.

The first derivative of the heat flow (W/g) versus temperature (°C) as 6CB is cooled shows similar peaks to the first derivative while the sample was heated. The larger peak appears during the transition from nematic to crystalline, while the smaller peak appears when the sample is transitioning from isotropic to nematic, as seen in Figure 20. The large peak is relatively broad in both, although slightly more narrow in Figure 20. However, in Figure 21, the peaks visible in the second derivative do not follow this pattern. The N-K phase transition, depicted by the leftmost peak, has more negative values than the I-N phase transition, which has the taller peak. Additionally, the second derivative peak of the crystalline-nematic cooling transition is negative, while the heating transition shows a positive peak. The third derivative of the heat flow (W/g) versus temperature (℃) during cooling also differs from the first and second derivatives, seen in Figure 22. The peaks that appear for the N-K and I-N phase transitions are similar heights, although the N-K peak contains more datapoints than the I-N peak.

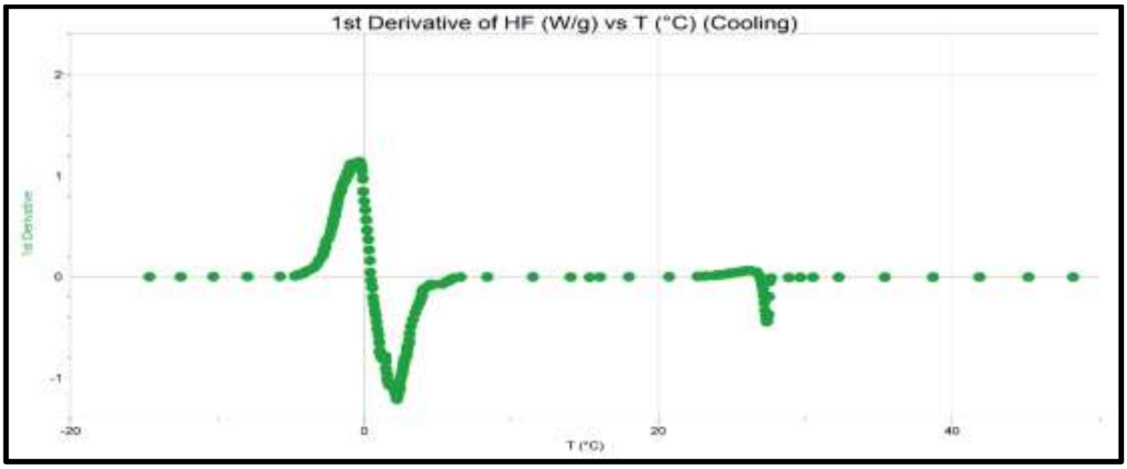

Figure 20. 1st Derivative of HF (W/g) vs T (℃) during the cooling of 6CB.

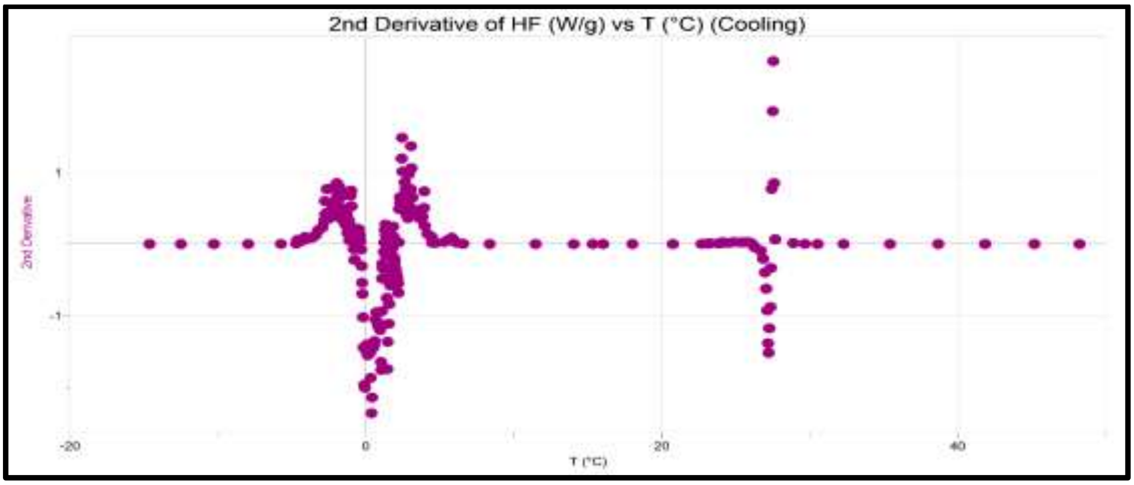

Figure 21. 2nd Derivative of HF (W/g) vs T (℃) during the cooling of 6CB.

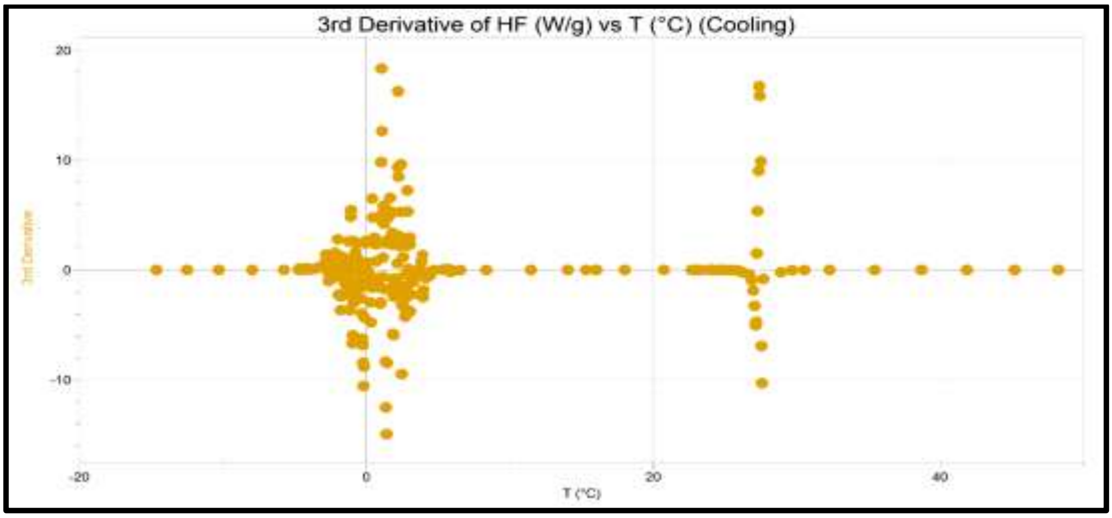

Figure 22. 3rd Derivative of HF (W/g) vs T (℃) during the cooling of 6CB.

All important peak details from Figures 4-25, as collected by DSC and analyzed with Logger Pro, are provided in Data Tables 1-8.

DATA TABLES

Table 1. Meanings of labels seen in Figures 4-8 and Tables 3 and 8.

	T_{KN}	T_{NI}	ΔH_{KN}	ΔH_{NI}	RN	ΔE
Meaning	Peak temperature for K-N transition	Peak temperature for N-I transition	Enthalpy for K-N transition	Enthalpy for N-I transition	Nematic Range	Change in internal energy

Table 2. Meanings of labels seen in Figures 9-12 and Tables 4 and 5.

	Ts	Te	ΔT	Cps	Cpe	Cpp	CpJ	ΔCp
Meaning	Starting temperature	End temperature	Change in temperature	Starting heat capacity	End heat capacity	Peak heat capacity	Wing jump	Change in heat capacity

Table 3. Heating and cooling phase transitions of 6CB.

	Heating					Cooling					
Sample	T_{KN} (°C)	T_{NI} (°C)	ΔH_{KN} (J/g)	ΔH_{NI} (J/g)	RN (°C)	T_{KN} (°C)	T_{NI} (°C)	ΔH_{KN} (J/g)	ΔH_{NI} (J/g)	RN (°C)	ΔE (J/g)
6CB	17.45	30.27	66.09	0.65	12.82	0.46	26.85	27.31	0.98	26.39	169.3

Table 4. Details of the heating of 6CB.

Heating 6CB										
Transition	Ts (°C)	Te (°C)	$T_{KN/NI}$ (°C)	ΔT (°C)	Cps (J/g°C)	Cpe (J/g°C)	Cpp (J/g°C)	CpJ (J/g°C)	ΔCp (J/g°C)	ΔH (J/g)
K-N	12.22	24.17	17.45	11.95	1.9	1.23	-15.56	0.67	17.22	66.09
N-I	28.73	33.56	30.27	4.83	1.7	1.52	1.26	0.18	0.34	0.65

Table 5. Details of the cooling of 6CB.

Cooling 6CB										
Transition	Ts (°C)	Te (°C)	$T_{KN/NI}$ (°C)	ΔT (°C)	Cps (J/g°C)	Cpe (J/g°C)	Cpp (J/g°C)	CpJ (J/g°C)	ΔCp (J/g°C)	ΔH (J/g)
K-N	28.90	22.68	26.85	6.22	-0.95	-0.80	-0.41	0.15	0.49	0.98
N-I	6.57	-5.74	0.46	12.31	-0.72	-0.78	7.11	0.06	7.87	27.31

Table 6. Time (in minutes) of phase transitions of 6CB.

	Heating	Cooling
Transition	Time (min)	Time (min)
K-N	4.25	15.10
N-I	4.85	12.44

Table 7. Details of the first, second, and third derivatives of heat flow plots.

nCB	Carbons in Tail	Molecular Weight (g/mol)	T_{NI} (°C)	Experimental T_{NI} (°C)	Nematic Range (°C)	ΔH (J/g)
4CB*	4	235.33	16	14.33	25.84*	9.02
5CB	5	249.36	35	35.75	29.75	0.37
6CB	6	263.38	29	30.27	12.82	0.65
7CB	7	277.41	42	42.45	12.45	12.20
8CB	8	291.44	40	40.25	18.6	3.13

Table 8. Details of the nematic phase transition during the heating of nCB LCs. (*data is from cooling)

		Heating		Cooling	
Plot	Derivative	K-N	N-I	N-I	K-N
HF (W/g) vs Time (min)	1st ((W/g)/min)	100520.000, -97910.847	25742.964, -12110.373	19014.004, -29273.309	8461.058
	2nd ((W/g)/min^{2})	2335.140	274.004, -226.800	372.615, -218.336	-169.387
	3rd ((W/g)/min^{3})	43.440, -36.933	-4.458	5.393	8.904, -10.575
HF (W/g) vs T (℃)	1st ((W/g)/℃)	0.019	-0.230	-0.446	1.140, -1.162
	2nd ((W/g)/℃^{2})	6.548	0.696, -0.589	2.553, -1.175	-2.360
	3rd ((W/g)/℃^{3})	17.955, -13.274	3.265, -10.309	16.743	18.352, -14.959

DISCUSSION

Using Table 8, the LCs from the nCB family were compared visually in the figures below. The literature and experimental values are similar, and show that there is an overall increase in the peak temperatures of the N-I phase changes of the nCB LCs as the value of n increases, as seen in Figure 23. As the molecular weights of the LCs increase (shown in Table 8), the peak temperature increases, because more energy is required to heat them. The LCs with an odd number of carbons in their tail have higher peak temperatures than the even LCs that directly precede or follow them in their “n” value.

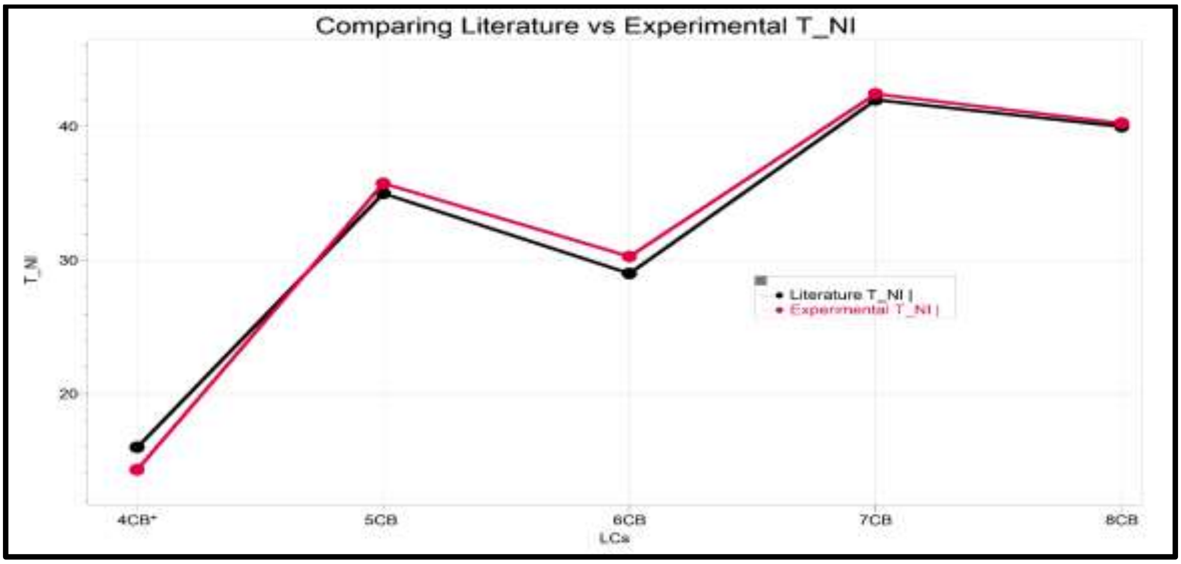

Figure 23. Comparing the Literature and Experimental T_NI values of LCs 4CB, 5CB, 6CB, 7CB, and 8CB.

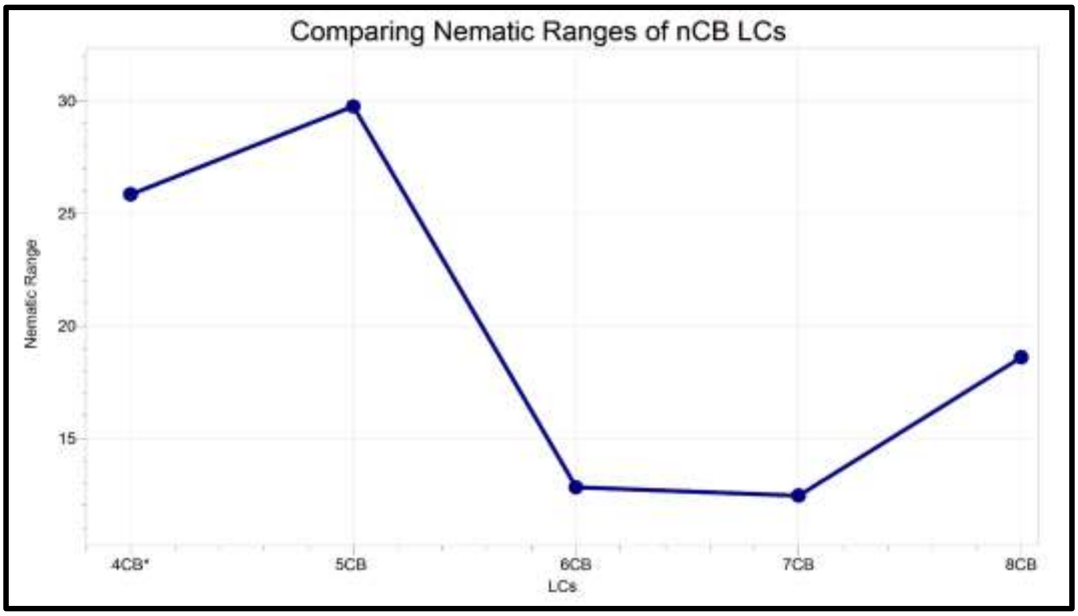

Figure 24. Comparing the Nematic Ranges of LCs 4CB, 5CB, 6CB, 7CB, and 8CB.

The LC 5CB has the highest nematic range out of the studied LCs, followed by 4CB, shown by Figure 24. 7CB has the lowest range, while the focus of this study, 6CB, has the second lowest nematic range during heating. However, 6CB’s nematic range during cooling is much wider, meaning its cooling nematic state would be better suited for LCD. The enthalpies of the N-I phase transition of each LC are seen in Figure 25. Looking at the LCs 5CB, 6CB, and 8CB, there is a slight increase in enthalpy as the “n” value increases, however, 4CB and 7CB do not follow this pattern. 7CB has the highest enthalpy, closely followed by 4CB.

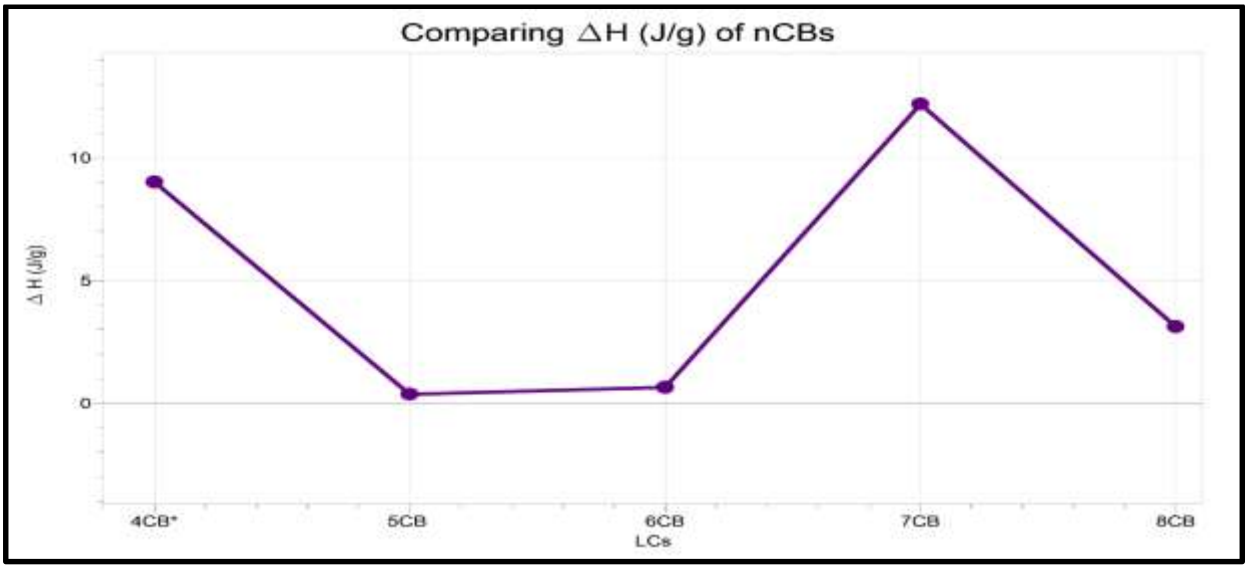

Figure 25. Comparing the ΔH (J/g) of LCs 4CB, 5CB, 6CB, 7CB, and 8CB during the N-I heating phase transition.

As illustrated in Figure 26, 6CB is rather intermediate when compared to 4CB, 5CB, 7CB, and 8CB. Each LC in the figure is a member of the nCB family, so they have the same basic structure except for the length of the tail, which corresponds to the LC’s “n” value. A molecule that contains more carbon atoms in its tail will be larger and have a higher molecular weight. Thus, 6CB is in-between the others in terms of size and molecular weight. The intermediate values of 6CB’s N-I peak temperature, nematic range, and N-I enthalpy show that 6CB could be used as an alternative to other LCs that may be employed for LCD, or other functions of LCs, such as being the key component in the color-changing rings known as “mood rings.” [22] Furthermore, studies indicate that a mixture of LCs can provide a wider, more practical nematic range. [23-26] Further research could be conducted to reveal the properties of a mixture between 6CB and other LCs, like 4CB or 5CB.

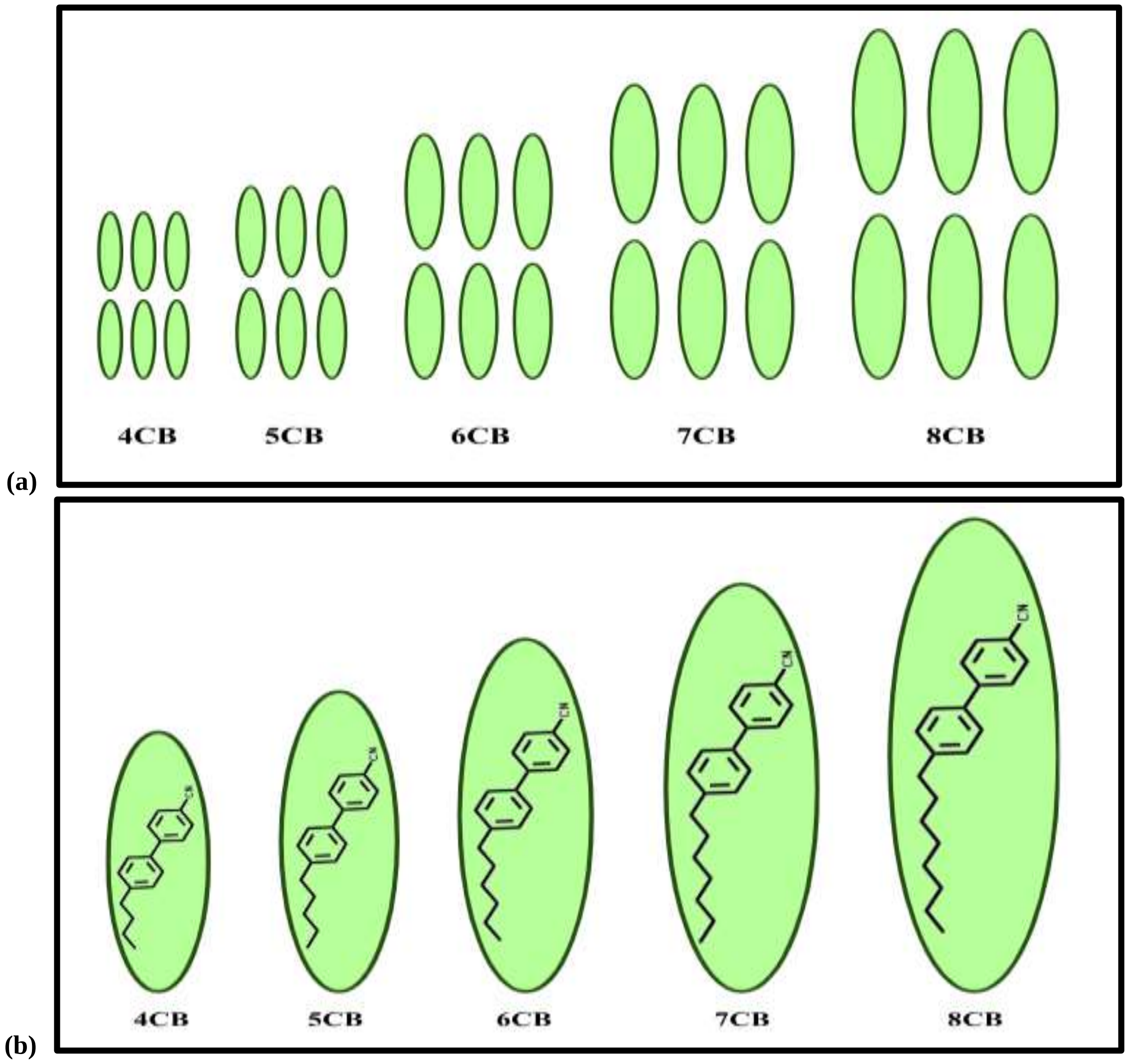

Figure 26. Comparing the sizes of 4CB, 5CB, 6CB, 7CB, and 8CB. Part (a) shows the LCs in the crystalline state, (b) shows how size increases with tail length.

CONCLUSION

This study reports the thermodynamic details of the 6CB liquid crystal, including its behavior as it is heated and cooled using DSC. The data retrieved through DSC was analyzed and interpreted through the use of Logger Pro in order to examine the phase transitions of the sample. During the heating of 6CB from -40 °C to 80 °C, one large endothermic peak is formed at 17.45 ℃, followed by a smaller peak at 30.27 ℃. During cooling from 80 °C to -40 °C, a small exothermic peak is formed at 26.85 ℃, after which the final peak is formed at 0.46 ℃. Additionally, the thermal speed, acceleration, and jerk of the sample were found by taking the first, second, and third derivatives of the heat flow. Details revealing properties of 6CB were compared to other members of the nCB family, including 4CB, 5CB, 7CB, and 8CB. One pattern emerged during the comparison of each LC’s peak temperature during the heating N-I phase transition. LCs with an odd number of carbons in their tail had higher peak temperatures than even LCs with an “n” value one digit higher or lower than the odd LC. However, no consistent pattern could be observed for the nematic ranges of the LCs, or for the enthalpy of their N-I phase transitions. In each category, the values found for 6CB were intermediate compared to those of the other LCs, likely due to its tail length being intermediate to the others. Among these values, it was found that 6CB has a nematic range of 12.82 ℃ while heating and 26.39 ℃ while cooling. This nematic range occurs around room temperature, which would make it useful in common environments. Overall, the results indicate that 6CB could be utilized as an alternative to other LCs, or possibly combined with a different LC to create another usable mixture for LCD.

ACKNOWLEDGEMENT

We would like to thank Professor John C. MacDonald from the Department of Chemistry and Biochemistry, WPI for his DSC instrument (Model MDSC 2920 from TA). Student would like to thank Dr. Dipti Sharma for supervising this research internship during summer 2023 and also to thank Emmanuel college for running Internship programs that help students to get internship experience.

REFERENCES

1. Mello, J., & Sharma, D. (2022). Effect of Reheating and Ramp Rates on Phase Transitions of 5OCB Liquid Crystal using Logger Pro. *International Journal of Research in Engineering and Science*, *10*(9), 218–236.
2. Sullivan, G. B., & Edmondson, C. (2008). Heat and temperature. *Continuing Education in Anesthesia Critical Care & Pain*, *8*(3), 104–107. https://doi.org/10.1093/bjaceaccp/mkn014
3. Win, D. (2006). States of matter-part I: the three common states: solid, liquid, gas. *AU Journal of Technology*, *9*(3), 153–157. https://repository.au.edu/items/39c47bb6-12f7-44a2-83f7-8bc32d9d79be
4. Andrienko, D. (2018). Introduction to liquid crystals. *Journal of Molecular Liquids*, *267*, 520–541. https://doi.org/10.1016/j.molliq.2018.01.175
5. Jasiurkowska-Delaporte, M., & Kolek, Ł. (2021). Nematic Liquid Crystals. Crystals, 11(4), 381. https://doi.org/10.3390/cryst11040381
6. Liu, K., Chen, D., Marcozzi, A., Zheng, L., Su, J., Pesce, D., Zajaczkowski, W., Kolbe, A., Pisula, W., Müllen, K., Clark, N. A., & Herrmann, A. (2014). Thermotropic liquid crystals from biomacromolecules. *Proceedings of the National Academy of Sciences of the United States of America*, *111*(52), 18596–18600. https://doi.org/10.1073/pnas.1421257111
7. McDonough, K., Vy, N. C. H., & Sharma, D. (2014). Existence of time lag in crystalline to smectic A (K–SmA) phase transition of 4-decyl-4-biphenylcarbonitrile (10CB) liquid crystal. *Journal of Thermal Analysis and Calorimetry*, *116*(3), 1515–1520. https://doi.org/10.1007/s10973-014-3812-5
8. Sharma, D., & Farah, K. (2016). Determination of latent heat of phase transitions of 8CB liquid crystal. *Trends in Physical Chemistry*, *16*, 17–24. https://www.researchgate.net/publication/315813762_Determination_of_latent_heat_of_phase_transitions_of_8CB_liquid_crystal
9. Tyson, J. (2023). How LCDs work. *HowStuffWorks*. https://electronics.howstuffworks.com/lcd.htm#:~:text=LCDs%20use%20these%20liquid%20crystals,as%20either%20thermotropic%20or%20lyotropic.
10. Sharma, D. (2009). Effect of alignment on the nematic to isotropic phase transition of bulk octylcyanobiphenyl brings possible solutions to liquid crystal display drawback. *Applied Physics Letters*, *94*(13). https://doi.org/10.1063/1.3112573
11. Seide, M., Doran, M., & Sharma, D. (2022). Analyzing nematic to isotropic (N-I) phase transition of NCB liquid crystals using Logger Pro. *European Journal of Applied Sciences*, *10*(3), 98–124. https://doi.org/10.14738/aivp.103.12373
12. Özgan, Ş., & Okumuş, M. (2011). Thermal and Spectrophotometric Analysis of Liquid Crystal 8CB/8OCB Mixtures. *Brazilian Journal of Physics*, *41*(2), 118–122. https://doi.org/10.1007/s13538-011-0034-1
13. Oweimreen, G. A., & Morsy, M. A. (2000). DSC studies on p-(n-alkyl)-p′-cyanobiphenyl (RCB's) and p-(n-alkoxy)-p′-cyanobiphenyl (ROCB's) liquid crystals. *Thermochimica Acta*, *346*(1–2), 37–47. https://doi.org/10.1016/s0040-6031(99)00411-6
14. Chiu, M. H., & Prenner, E. J. (2011). Differential scanning calorimetry: An invaluable tool for a detailed thermodynamic characterization of macromolecules and their interactions. *Journal of Pharmacy and Bioallied Sciences*, *3*(1), 39. https://doi.org/10.4103/0975-7406.76463
15. Sharma, D., MacDonald, J. M., & Iannacchione, G. S. (2006). Thermodynamics of activated phase transitions of 8CB: DSC and MC calorimetry. *Journal of Physical Chemistry B*, *110*(33), 16679–16684. https://doi.org/10.1021/jp062862d
16. Devadiga, D., & Ahipa, T. (2022). A review on the emerging applications of 4-cyano-4′-alkylbiphenyl (nCB) liquid crystals beyond display. *Materials Science and Engineering: B*, *275*, 115522. https://doi.org/10.1016/j.mseb.2021.115522
17. Sharma, D. M. (2010). Non-isothermal kinetics of melting and nematic to isotropic phase transitions of 5CB liquid crystal. *Journal of Thermal Analysis and Calorimetry*, *102*(2), 627–632. https://doi.org/10.1007/s10973-010-0837-2
18. Doran, M., Seide, M., & Sharma, D. (2022). Reporting Strange and Unique Behavior of 4CB Liquid Crystal using Logger Pro. *International Journal of Research in Engineering and Science*, *10*(5), 27–41.
19. Sharma, D., & Farah, K. (2016). A review of nematic liquid crystals. *Trends in Physical Chemistry*, *16*, 47–52. https://www.researchgate.net/publication/315813501_A_review_of_nematic_liquid_crystals_Trends_in_Physical_Chemistry
20. Mello, J., & Sharma, D. (2022). Details of Nematic Phase Transition and Nematic Range of 5OCB Liquid Crystal using Logger Pro. *International Journal of Research in Engineering and Science*, *10*(9), 197–217.
21. Rajak, P., Nath, L. K., & Bhuyan, B. (2019). Liquid crystals: an approach in drug delivery. *Indian Journal of Pharmaceutical Sciences*, *81*(1). https://doi.org/10.4172/pharmaceutical-sciences.1000474

22. Helmenstine, A. M., PhD. (2019). How do mood rings work? *ThoughtCo*. https://www.thoughtco.com/mood-rings-thermochromic-liquid-crystals-608013
23. Doran, M., & Sharma, D. (2023). Effect of Ramp Rates on Phase Transitions of a Next Generation ‘Binary Liquid Crystal System” (BLCS) 5CB+7CB. *International Journal of Engineering Inventions*, *12*(1), 291–306.
24. Doran, M., & Sharma, D. (2022). Melting and Nematic Phase Transitions of a Next Generation “Binary Liquid Crystal System (BLCS)” 5CB+7CB using Logger Pro. *International Journal of Research in Engineering and Science*, *10*(12), 462–483.
25. Seide, M., & Sharma, D. (2023). Observance of Multiple Melting and Nematic Phase Transitions in A Next Generation “Quaternary Liquid Crystal System” (QLCS). *Global Journal of Materials Science and Engineering*, *5*(2). https://doi.org/10.36266/GJMSE/151
26. Seide, M., & Sharma, D. (2023). Reporting Phase Transitions of a New Generation “Tertiary Liquid Crystal System” (TLCS) using Logger Pro. *SSRG International Journal of Applied Physics*, *10*(1), 22–33. https://doi.org/10.14445/23500301/ijap-v10i1p104